High Count Rate First-Pass Radionuclide Angiography Using a Digital Gamma Camera

Rami Gal, Raymond P. Grenier, John Carpenter, Donald H. Schmidt, and Steven C. Port

Nuclear Cardiology Laboratory, Mount Sinai Medical Center, University of Wisconsin Medical School, Milwaukee Clinical Campus, Milwaukee, Wisconsin

In this study, first-pass radionuclide angiography (FPRNA) was performed using a digital single-crystal gamma camera. Twenty-nine men and six women (ages 43–80, mean 61 yr) underwent FPRNA in the supine position immediately prior to cardiac catheterization. Total counts/sec in the whole field-of-view in the right ventricular phase were 150,352 ± 26,006. Background uncorrected counts in the representative cycle were 7,651 ± 2,527 at end-diastolie and 4,904 ± 2,314 at end-systolie. A linear correlation between FPRNA left ventricular (LV) ejection fraction and contrast LV ejection fraction gave an r = 0.95 with an s.e.e. of 0.05. Analyses of intra- and interobserver variability gave r = 0.99 and 0.98 and an s.e.e. of 0.02 and 0.03, respectively. Spearman-Rank correlation coefficients between FPRNA and contrast angiographic wall-motion scores were >0.8 for all walls, while sensitivity/specificity were 0.86/0.90, 0.76/1.00, 0.76/1.00 for anterior, apical, and inferior wall-motion abnormalities, respectively. We conclude that satisfactory counting statistics for FPRNA can be obtained with a digital gamma camera, and that accurate and reproducible measurements of global and regional left ventricular function can be obtained with this technique.

First-pass radionuclide angiography (FPRNA) offers several advantages over equilibrium radionuclide angiography in the evaluation of ventricular function. FPRNA can be performed and quantitative data obtained in multiple views. The short imaging time lends itself to the evaluation of very transient phenomena and minimizes the need for patient cooperation (*1*). The use of radionuclides with ultra-short half-lives permits multiple, rapid, sequential acquisitions (*2,3*) and simultaneous radionuclide ventriculography and perfusion imaging (*4*).

In clinical practice, FPRNA has essentially been the province of the multicrystal gamma camera. The multicrystal gamma camera reliably provides acquisition count rates that are adequate for first-pass imaging (*5*). Two major disadvantages of the multicrystal gamma camera are its poorer spatial and energy resolution compared to single-crystal cameras and its inability to

adequately perform the entire gamut of both cardiac nuclear studies and general nuclear medicine procedures (*5,6*).

The practical appeal, then, of a high count rate single-crystal camera is that it could perform adequate FPRNA as well as the entire spectrum of nuclear studies. In this study, we present a comprehensive investigation of the application of such a high count rate fully digital single-crystal gamma camera to first-pass radionuclide angiography.

MATERIALS AND METHODS

Study Design and Patient Population

Two groups of patients were studied. Both groups underwent cardiac catheterization, contrast ventriculography, and coronary arteriography because of known or suspected coronary artery disease or valvular heart disease.

Both groups of patients had first-pass radionuclide angiography performed immediately prior to cardiac
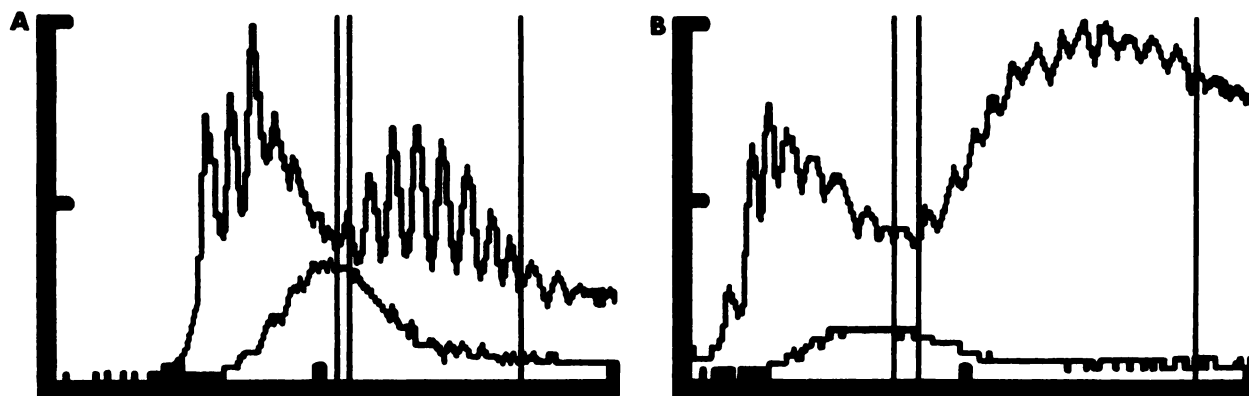
FIGURE 1
Typical examples of time-activity curves from an LV ROI and background ROI in patient with normal (A) and depressed (B) LV function. Cursors represent (left to right) background frame for normalization, beginning of LV phase and end of LV phase for analysis

catheterization. All patients were studied in the supine position in the holding area of the catheterization laboratory after premedication.

The radionuclide results from Group A patients were analyzed both prospectively and retrospectively to establish in an ongoing fashion: (a) necessary hardware modifications; (b) appropriate acquisition parameters; and (c) software for data processing. That process led to several different computer programs for first-pass data processing, all of which were modified according to the results of the contrast ventriculography. The data from Group A are not presented in this report. Once finalized, the hardware and software modifications and the standardized approach of data acquisition were prospectively applied to Group B patients. The results of the prospective study form the basis of this report.

Group A was composed of 28 men and seven women ranging in age from 46 to 78 yr (mean 61). Within Group A, 30 patients had coronary artery disease, two had valvular heart disease and three had no demonstrable heart disease. Their ejection fractions ranged from 0.24 to 0.82.

Group B initially included 40 patients, five of whom were subsequently excluded because of rapid atrial fibrillation (2), technically inadequate radionuclide angiograms (2), and a technically inadequate contrast ventriculogram (1). The remaining 35 patients in Group B included 29 men and six women ranging in age from 43 to 80 yr (mean 61). Thirty-one Group B patients had coronary artery disease, three had valvular heart disease and one had no demonstrable heart disease. All patients were in sinus rhythm at the time of study.

Gamma Camera Hardware

All FPRNA was performed with a fully digital, small field-of-view (7⅞ in. diam) portable single-crystal gamma camera*. Initially, the commercially provided

1-in.-thick, low-energy, ultra-high sensitivity collimator (sensitivity 11.0×10^{-4}, resolution full width at half maximum (FWHM) = 19.4 mm at 3 in.) was used. During the course of the Group A study a new collimator was designed by one of the investigators (R.P.G.). That collimator is 1½ in. thick. It has a row and column orientation of the holes. The hole diameter is 6.32 mm, the center-to-center spacing is 6.9 mm, and the thickness is 41.6 mm. It is designed such that with appropriate software modifications and camera calibrations each collimator hole is aligned with an individual pixel. All Group B patients were studied with the latter collimator. Nonuniformity corrections and calibration were performed automatically by the computer according to locally derived isotope maps and tables.

Radionuclide Acquisition Protocol

All patients were studied in the supine position. For most patients, a 1¼-in., 20-gauge Teflon catheter was placed in an external jugular vein while in some patients, because of inadequate neck veins, a 1¾-in., 18-gauge Teflon catheter was placed in an antecubital vein.

Twenty-five to thirty millicuries technetium-99m diethylenetriaminepentaacetic acid ([^{99m}Tc]DTPA) in less than 1 ml saline were loaded into an extension tubing attached to the catheter and the isotope bolus was flushed in with 20 ml of saline. The gamma camera detector was positioned in a 20°–30° right anterior oblique projection. One millicurie of [^{99m}Tc]DTPA was injected for proper positioning. Acquisition was started just prior to the radionuclide injection. Counts were accumulated for 30 sec in frame mode using a frame time of 0.03 sec and a $32 \times 32 \times 8$ matrix (0.68 cm/pixel). The energy window was 119–161 keV (±15%). Data were acquired directly onto the hard disk and subsequently transferred to floppy disk for storage and processing.
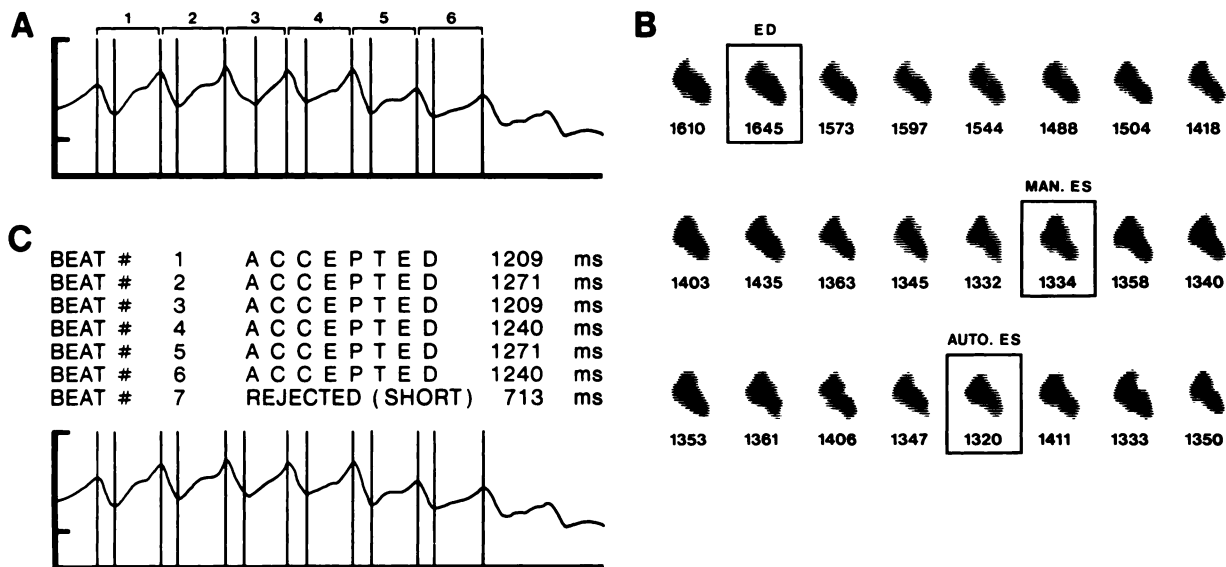
FIGURE 2
Beat editing. A: In this time-activity curve the computer chosen end-systolic frame of third beat results in systolic time interval that is obviously longer than others despite constant heart rate. B: By reference to individual frame images and their corresponding counts shown below, computer chosen (AUTO. ES) end-systolic frame is replaced with manually chosen (MAN. ES) one. C: Corrected time-activity curve
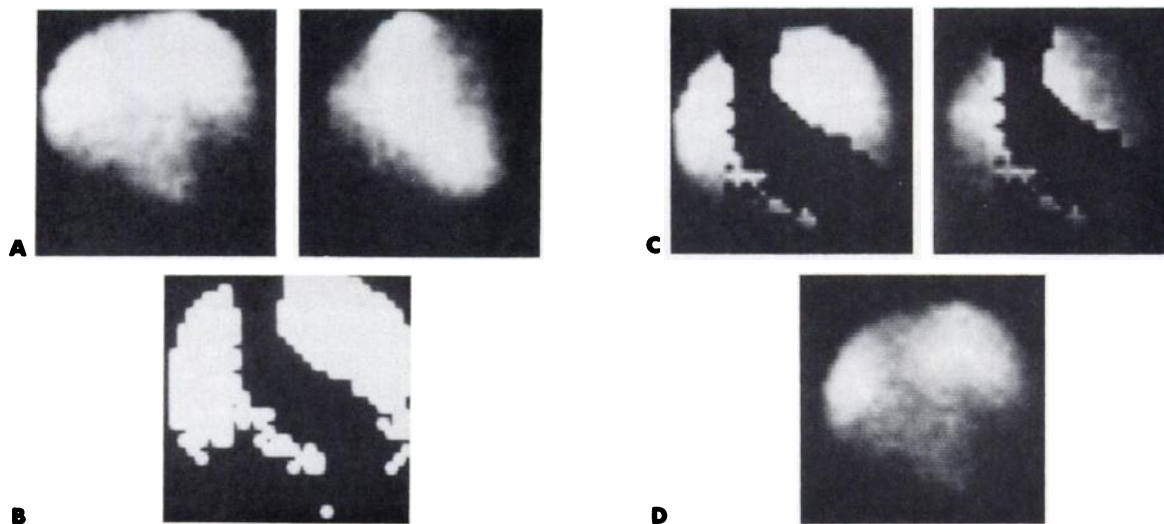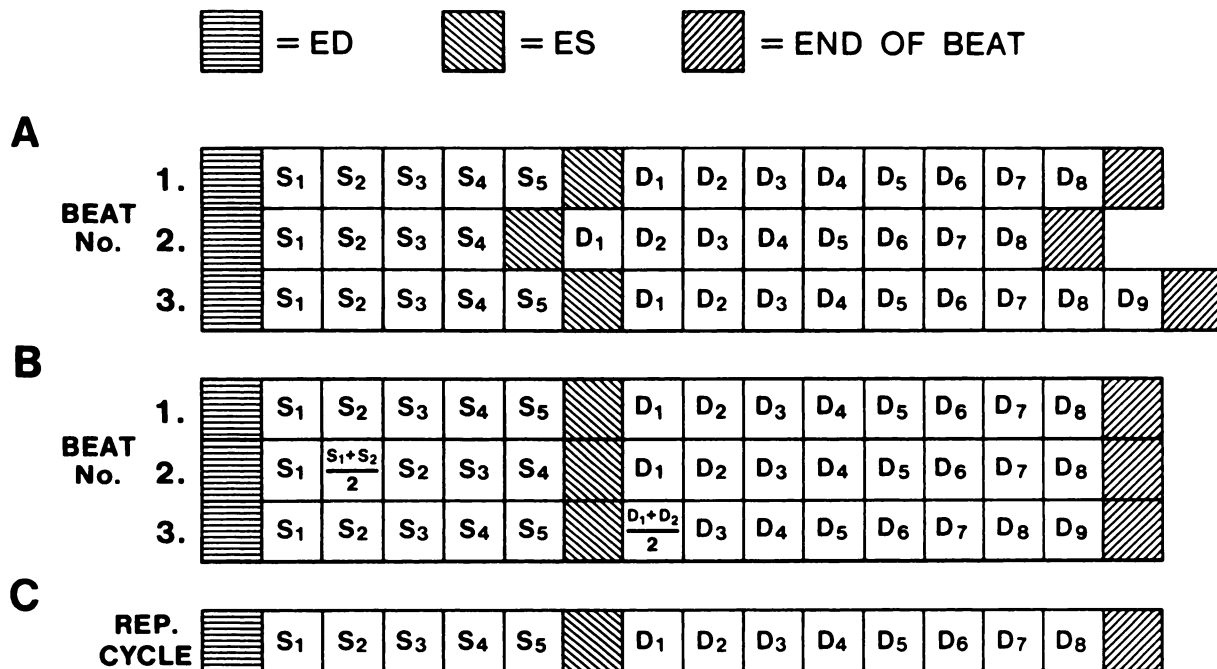

FIGURE 3
Lung background method (D_0 and D_1). A: Summed background frame (left) and end-diastolic frame of LV representative cycle (right). B: LV frame in A is subtracted from background frame to create a mask of LV and background regions. C: That mask is applied to summed background frame (left) and to end-diastolic LV frame, and counts in background ("lung") region are determined in each image. Ratio of background counts in the two images gives background washout factor. D: Summed background frame in A is then multiplied by washout factor to give image in D that is then used to correct all frames of the representative cycle

Radionuclide Data Processing

Data processing was performed using the computer and software of the gamma camera. The individual 0.03-sec frames were grouped into 0.5-sec frames for an initial visual identification of the left ventricular (LV) phase of the study. Then, using the digitized R wave of the ECG to identify end-diastole, the original 0.03-sec frames within the LV phase were cyclically added to create a crude uncorrected representative cycle. A nine-point spatially smoothed end-diastolic frame from that representative cycle was used to manually draw an LV region of interest (ROI). The latter was used to create a

FIGURE 4
Beat alignment. A: Three representative beats are displayed diagrammatically with consecutive systolic (S) and diastolic (D) frames numbered. Beat 2 has shorter systolic interval than Beats 1 and 3 while Beat 3 has longer diastolic interval than Beats 1 and 2. B: Systolic interval of Beat 2 is lengthened while diastolic interval of Beat 3 is shortened as shown in diagram. C: Final aligned representative cycle

histogram of the entire 30 sec of the study. From that histogram, the beginning and end of the LV phase were again identified and a frame prior to the LV phase was chosen for subsequent background correction (Fig. 1). The end-diastolic (ED) and end-systolic (ES) frames from the LV phase were automatically identified by the computer according to sequential peak and rough counts. The program also provided automatic beat rejection based on R-R interval criteria and manual beat editing. The latter allowed changes in the selection of ED and ES frames based on frame counts, frame images, and the time-activity curve as well as determination of the total number of beats accepted or rejected (Fig. 2).

For background correction, a summed background frame was created from a number of frames equal to the number of beats in the representative cycle starting with the previously identified pre-LV phase frame (see above). The ED frame of the representative cycle was subtracted from the summed background frame leaving a background mask. The count ratio between the background frame and the ED frame (counting only masked areas) was used to calculate the background washout factor which was then used to normalize the background frame (Fig. 3).

To create the final representative cycle, the end-diastolic frames of the accepted beats were summed as were the end-systolic frames. The frames during systole and diastole were aligned according to the average systolic and diastolic intervals (Fig. 4). By adding or condensing frames (average of two neighboring frames) the final aligned representative cycle always had the correct ED and ES while intermediate frames may have been slightly modified. The normalized background frame corrected by the washout factor was then subtracted from each frame of the representative cycle. After background correction and application of a median filter, a Fourier phase analysis of the aligned representative cycle was performed. The previously drawn LV ROI was then applied to the ED image of the corrected representative cycle and to the phase image. At this point the operator had to adjust the LV ROI, if necessary, to conform to the borders of the phase image. If the LV ROI was adjusted, the entire beat selection process was repeated using the new ROI. The ejection fraction EF was calculated from the final background corrected representative cycle where LVEF = (ED counts − ES counts)/ED counts.

Contrast Angiography

Left heart catheterization and coronary arteriography were performed using standard techniques. Contrast ventriculography was performed at 30 frames/sec in the 30° right anterior oblique projection using 30–50 ml of diatrizoate meglumine. Selective coronary arteriography was performed in multiple views. Left ventric-
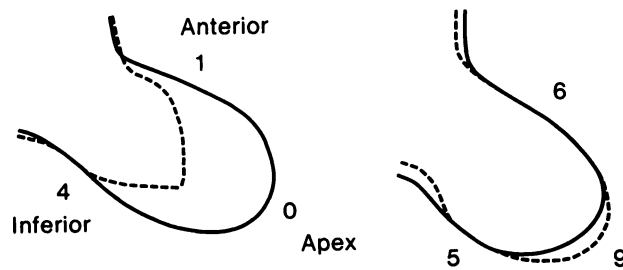
FIGURE 5
Regional wall motion scoring. Two examples of end-diastolic (solid) and end-systolic (broken) perimeters and accompanying scores. 0 = Normal; 1–3 = Hypokinesia; 4–6 = Akinesia; 7–9 = Dyskinesia

ular volumes and ejection fractions were calculated using the Kennedy modification of the single-plane area-length method of Sandler et al (7). Only sinus beats were selected.

Analysis of Regional Wall Motion

Both radionuclide and contrast cineventriculograms were analyzed using a semiquantitative ten-point scoring system that described both the severity and extent of a wall motion abnormality. In that system, 0 = normal wall motion and 9 = dyskinesia of an entire wall. Three walls were so scored from the RAO projection, the anterior, apical and inferior walls (Fig. 5). The FPRNA cineventriculograms were interpreted blindly and independently by two of the authors. Each observer independently recorded scores for all segments. The final score used for comparison with the contrast ventriculographic scores was taken as the average of the scores of the two observers. The same two authors scored the contrast ventriculograms by consensus without knowledge of the FPRNA results.

Statistical Methods

Paired observations were analyzed using a Students t-test and a least squares fit for determination of a regression equation. A Spearman rank correlation was used to compare the contrast angiographic wall-motion scores to those from FPRNA. Significance of differences was determined at the $p < 0.05$ level.

RESULTS

Radionuclide Counting Statistics

A 25–30 mCi bolus (FWHM 0.8 ± 0.3 sec in the superior vena cava) resulted in an average whole field-of-view count rate of 150,352 ± 26,006 cps (range 70,000–189,000) during the right ventricular phase and 124,628 ± 26,527 cps (range 53,000–175,000) during the left ventricular phase. Within the LV ROI, peak background-uncorrected counts at ED averaged

TABLE 1
Radionuclide and Contrast LVEF in 35 Patients

| Patient no. | Sex | Age (yr) | LVEF | | Contrast angiography |
| | | | Radionuclide | | |
			Uncorrected	Corrected	
1	M	61	0.44	0.76	0.75
2	M	58	0.37	0.66	0.68
3	M	62	0.47	0.65	0.68
4	M	65	0.45	0.71	0.68
5	M	51	0.39	0.82	0.75
6	F	73	0.28	0.45	0.49
7	M	43	0.42	0.71	0.71
8	F	68	0.53	0.74	0.84
9	F	66	0.53	0.71	0.72
10	M	61	0.23	0.33	0.36
11	M	71	0.33	0.42	0.52
12	M	80	0.16	0.24	0.22
13	M	71	0.23	0.45	0.26
14	M	60	0.39	0.68	0.70
15	F	73	0.32	0.56	0.58
16	M	73	0.43	0.68	0.68
17	M	70	0.19	0.24	0.24
18	M	57	0.35	0.68	0.66
19	M	53	0.35	0.65	0.73
20	M	45	0.39	0.76	0.72
21	M	53	0.41	0.59	0.62
22	M	56	0.26	0.38	0.44
23	M	49	0.32	0.46	0.52
24	M	74	0.42	0.69	0.74
25	M	46	0.42	0.71	0.70
26	M	55	0.51	0.73	0.77
27	M	69	0.25	0.44	0.38
28	M	52	0.38	0.57	0.54
29	M	58	0.36	0.69	0.66
30	M	62	0.34	0.60	0.65
31	M	59	0.44	0.69	0.68
32	F	59	0.36	0.55	0.50
33	F	55	0.43	0.70	0.75
34	M	71	0.29	0.39	0.33
35	M	65	0.10	0.14	0.18

45,529 ± 10,776 cps (range 21,000–73,000). An average of 6.5 (range 4–9) beats comprised the representative cycle. Background uncorrected ED and ES frame counts in the representative cycle were 7,651 ± 2,527 and 4,904 ± 2,314, respectively. The ratio of background counts to uncorrected ED counts was 0.42 ± 0.09. Background corrected ED and ES counts in the representative cycle were 4,523 ± 1,951 and 2,127 ± 1,898, respectively.

Ejection Fraction Results

The individual uncorrected and background corrected radionuclide ejection fractions and the contrast ejection fractions are listed in Table 1. The mean contrast left ventricular ejection fraction (LVEF) was 0.59 ± 0.18 (range 0.18–0.84) and the mean background corrected FPRNA LVEF was 0.58 ± 0.17 (range 0.14–0.82). A paired t-analysis showed no significant difference between the contrast and radionuclide ejection fractions. Correlation and linear regression ana-
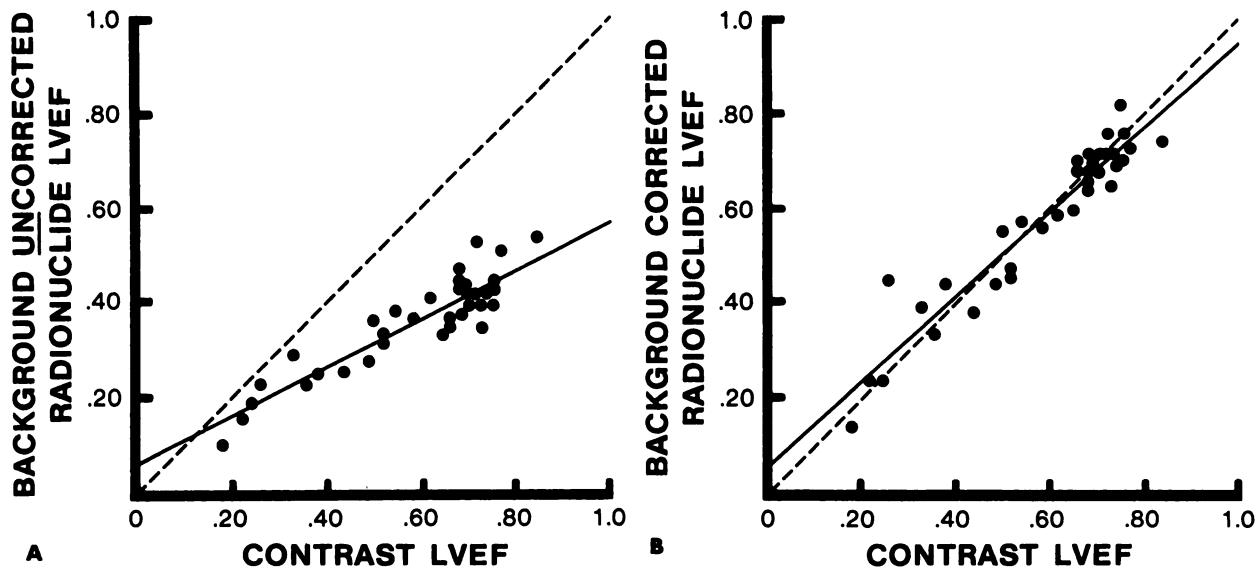
FIGURE 6

Linear regressions between contrast LVEF and FPRNA LVEF without (A) and with (B) background correction. A: y = 0.51x + 0.06; r = 0.91; s.e.e. = 0.04. B: y = 0.90x + 0.05; r = 0.95; s.e.e. = 0.05
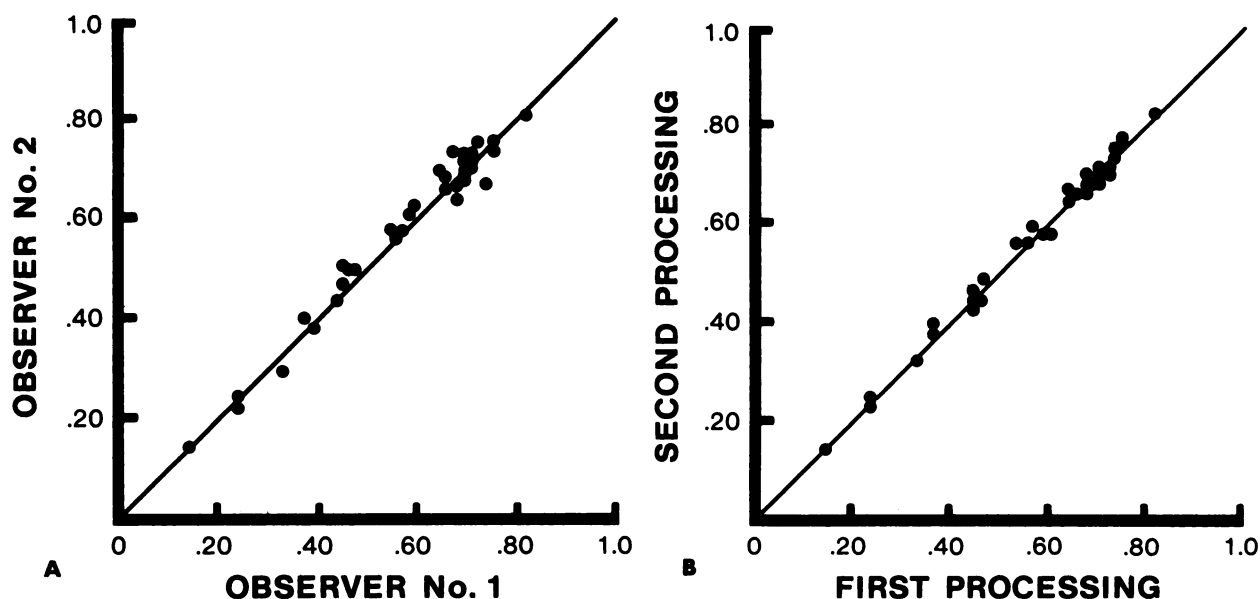

FIGURE 7

Interobserver (A) and intraobserver (B) variability of FPRNA LVEF determinations. A: y = 0.99x + 0.01; r = 0.98; s.e.e. = 0.03. B: y = 0.98x + 0.01; r = 0.99; s.e.e. = 0.02

lyses yielded an r of 0.95 with a slope of 0.9 (Fig. 6). Intraobserver and interobserver variations in the determination of the radionuclide LVEF are shown in Fig. 7. Excellent correlations were obtained with r values of 0.99 and 0.98 and standard errors of the estimate of 0.02 and 0.03 for the intra- and interobserver differences, respectively.

Wall-Motion Analysis

Examples of contrast and FPRNA ventriculograms are shown in Fig. 8. A total of 105 segments were graded on both the contrast and radionuclide ventriculograms. There were 48/105 (46%) unequivocally abnormal (wall-motion score ≥ 1.0) segments and 57/105 (54%) normal segments on the contrast ventriculograms. The radionuclide scores correctly identified 38 of the 48 abnormal segments (79%) and were normal in 55 of the 57 normal segments (96%). As seen in Table 2, the radionuclide sensitivity for anterior wall motion abnormalities was higher than the sensitivities for apical and inferior wall-motion abnormalities although the differences were not significant. A Spearman rank cor-
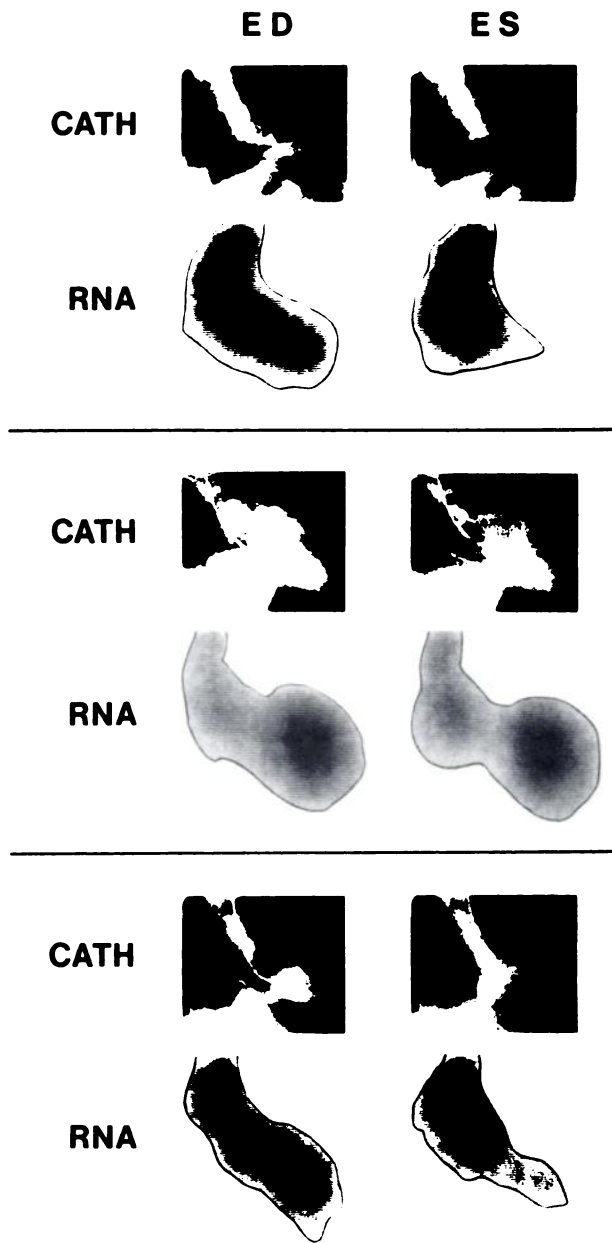
ED   ES

CATH

RNA

CATH

RNA

CATH

RNA

FIGURE 8
Examples of contrast and FPRNA ventriculograms. Normal LV (top). Large anteroapical LV aneurysm (middle). LV with inferobasal akinesia on contrast study was interpreted as hypokinetic on FPRNA study (bottom)

TABLE 2
Sensitivity and Specificity of RNA Wall-Motion Analysis

Item	Anterior	Apex	Inferior	Total
Sensitivity	12/14 (86%)	13/17 (76%)	13/17 (76%)	38/48 (79%)
Specificity	19/21 (90%)	18/18 (100%)	18/18 (100%)	55/57 (96%)
Spearman rank correlation coefficient	0.81	0.82	0.86	—
Linear correlation	0.86	0.82	0.77	—

TABLE 3
Contrast and Radionuclide Wall-Motion Abnormalities by Severity

RNA wall motion	Contrast ventriculographic wall motion					
	Anterior		Apex		Inferior	
	Akin/ Dysk	Hypo	Akin/ Dysk	Hypo	Akin/ Dysk	Hypo
Akin/Dysk	3	0	4	0	4	0
Hypo	1	8	2	7	5	4
Normal	0	2	0	4	0	4

of hypokinetic apical segments and 50% of hypokinetic inferior segments.

DISCUSSION

Cardiac blood-pool imaging can be performed using either the first-pass or gated equilibrium technique. Both techniques provide accurate and reproducible measurements of global and regional ventricular function at rest and during exercise (8–10). However, each technique has its own particular advantages and disadvantages. Ideally, the technique of choice should depend on the clinical questions at hand and the appropriateness of each method for a given individual. Unfortunately, the choice of techniques is more often determined by the equipment available rather than the relative merits of the two techniques in a given patient. The first-pass technique has traditionally been performed with a multicrystal gamma camera while the majority of laboratories have general-purpose single-crystal gamma cameras. Although the latter can be used to perform so called gated first-pass studies (11), to date, only the multicrystal gamma camera reliably provided the count rates necessary for first-pass imaging. A single-crystal gamma camera that could perform general nuclear medicine studies and the entire gamut of cardiovascular nuclear studies including high count rate first-pass studies would be of obvious benefit.

Counting Statistics

In this study, we report the counting statistics and clinical accuracy obtainable during first-pass radionu-

relation between the radionuclide and contrast wall motion scores gave coefficients of 0.81, 0.82 and 0.86 for the anterior, apical, and inferior walls, respectively. In Table 3, the sensitivities are related to both the severity and location of the wall motion abnormality. It can be seen that the RNA was always abnormal when the contrast study showed akinesia or dyskinesia. However, when the contrast study showed hypokinesia, the RNA was normal 34% of the time. Only 20% of hypokinetic anterior segments were missed compared to 36%

clide angiography using a digital single-crystal gamma camera. With a small field-of-view (7⅞-in. diam) camera and a 25–30 mCi bolus we achieved count rates of 150,352 ± 26,006 cps during the right ventricular phase of the study. The highest count rate was 189,000 cps. As a result, the end-diastolic and end-systolic counts during the left ventricular phase were adequate for quantitative analysis of left ventricular function. Those statistics compare favorably with those obtained with a multicrystal gamma camera despite use of the RAO view which results in lower count rates than those seen in the anterior view, a narrower energy window, and the lack of deadtime correction that is typically used in the multicrystal gamma camera software (*12*).

The high count rates seen in this study are due to several hardware and software modifications not present on previous generations of single-crystal cameras. High quantum efficiency (>30%) photomultiplier tubes enhance the ability to rapidly determine the x,y coordinates of the scintillation events. A fast hardware array processor is integrated with the front end to reduce count losses sustained in transferring the signals from camera to computer. A shortened integration circuit time, and fast spatial and energy corrections also minimize count losses. Finally, our own collimator modification and its link to the acquisition software improve spatial resolution and increase the counting efficiency by 10%.

Ejection Fraction Measurements

The correlation coefficient between the radionuclide and contrast LVEF was 0.95 while the slope of the regression equation was 0.9 and the s.e.e. 0.05. These results are similar to those obtained with a multicrystal camera (*10,13,14*). An excellent correlation was also seen between the background uncorrected radionuclide data and the contrast LVEF. The latter is testimony to the inherent accuracy of the software used to create the representative cycle. We believe that the ability to interact with the computer for both beat selection and beat editing and the alignment of beats according to the true end-diastoles and end-systoles are particularly important in maintaining data integrity. The alignment process preserves the true end-diastolic counts and end-systolic counts of each beat while allowing intermediate frame counts to vary according to a nearest-neighbor averaging technique (Fig. 3).

Interobserver and intraobserver variability were minimal in this study with correlation coefficients of 0.98 and 0.99, respectively. In large part, the lack of variability was due to the use of the phase image to guide the operator in determining the final LV ROI. In 10% of the cases the phase image was not used because of regional akinesis or inadequate statistics. In those cases, the LV ROI was determined manually from the end-diastolic and end-systolic images.

Regional Wall Motion

The semiquantitative wall-motion scoring system used in this study proved sensitive (79%) and highly specific (96%) for the detection of wall-motion abnormalities seen on contrast ventriculography. Spearman rank correlation coefficients between FPRNA and contrast wall-motion scores were >0.8 for the three walls analyzed. There was, however, a consistent underestimation by FPRNA. The sensitivity for individual walls was 86% for the anterior wall and 76% for the inferior wall and apex (p = N.S., χ^2). Although akinetic or dyskinetic segments on contrast ventriculography were all designated as abnormal on FPRNA, underestimation of severity did occur, primarily of the inferior wall. Of the hypokinetic walls on the contrast studies, 34% were incorrectly classified as normal on the FPRNA study, with the inferior wall again showing the most frequent underestimation. Previous investigators have noted lower sensitivities for inferior wall-motion abnormalities using FPRNA (*13,15*). The latter has been attributed to oversubtraction of background (RV counts present during the LV phase) and to interference by the mitral valve apparatus and papillary muscle (*13,15*). The descending aorta may also contribute to that problem.

Clinical Implications

The results of this study should be of interest to laboratories performing cardiac imaging. The data show that adequate statistics for accurate, reproducible measurements of left ventricular ejection fraction and analysis of regional wall motion using the first-pass technique can be obtained with a single-crystal camera. As such, any nuclear laboratory can perform either first-pass or equilibrium blood-pool imaging with one camera and the choice of techniques can depend on which one is clinically most appropriate for a given patient. Furthermore, the same camera can be used for other cardiac imaging such as thallium-201 perfusion and [99mTc]pyrophosphate infarct imaging. It is important to recognize that the results obtained in this study are dependent upon the use of the collimator and the data processing techniques described in this study (all of which are now available commercially) and may not be reproduced without them. It is also important to recognize that our results required 25–30 mCi boluses and would therefore limit the number of acquisitions. In the future, further hardware/software modifications and short-lived radionuclides such as gold-195m may provide higher count rates with lower radiation doses.

FOOTNOTE

* Apex 215, Elscint, Inc., Boston, MA.

ACKNOWLEDGMENTS

REFERENCES

1. Ashburn WL, Schelbert HR, Verba JW: Left ventricular ejection fraction—A review of several radionuclide angiographic approaches using the scintillation camera. *Prog Cardiovasc Dis* 20:267–284, 1978
2. Dymond DS, Elliott AT, Flatman PW, et al: The clinical validation of gold-195m: A new short half-life radiopharmaceutical for rapid, sequential, first pass angiocardiography in patients. *J Am Coll Cardiol* 2:85–92, 1983
3. Mena I, Narahara KA, de Jong R, et al: Gold-195m, an ultra-short-lived generator-produced radionuclide: Clinical application in sequential first pass ventriculography. *J Nucl Med* 24:139–144, 1983
4. Wackers FJT, Stein R, Ptylik L, et al: Gold-195m for serial first pass radionuclide angiocardiography during upright exercise in patients with coronary artery disease. *J Am Coll Cardiol* 2:497–505, 1983
5. Budinger TF, Rollo FD: Physics and instrumentation in nuclear medicine. *Prog Cardiovasc Dis* 20:19–54, 1977
6. Borer JS, Bacharach SL, Green MV, et al: Assessment of ventricular function by radionuclide angiography: Applications and results. *Cardiology* 71:136–161, 1984
7. Kennedy JW, Baxley WA, Figley MM, et al: Quantitative angiocardiography. I. The normal left ventricle in man. *Circulation* 34:272–278, 1966
8. Folland ED, Hamilton GW, Larson SM, et al: The radionuclide ejection fraction: A comparison of three radionuclide techniques with contrast angiography. *J Nucl Med* 18:1159–1166, 1977
9. Okada RD, Kirshenbaum HD, Kushner FG, et al: Observer variance in the qualitative evaluation of left ventricular wall motion and the quantitation of left ventricular ejection fraction using rest and exercise multigated blood pool imaging. *Circulation* 61:128–136, 1980
10. Scholz PM, Rerych SK, Moran JF, et al: Quantitative radionuclide angiocardiography. *Cathet Cardiovasc Diagn* 6:265–283, 1980
11. Winzelberg GG, Boucher CA, Pohost GM, et al: Right ventricular function in aortic and mitral valve disease: Relation of gated first-pass radionuclide angiography to clinical and hemodynamic findings. *Chest* 79:520–528, 1981
12. *Nuclear Cardiology Reference Manual for Use with System Seventy-Seven*, Baird Corporation, Nuclear Division:II-2
13. Bodenheimer MM, Banka VS, Fooshee CM, et al: Quantitative radionuclide angiography in the right anterior oblique view: Comparison with contrast ventriculography. *Am J Cardiol* 41:718–725, 1978
14. Marshall RC, Berger HJ, Costin JC, et al: Assessment of cardiac performance with quantitative radionuclide angiocardiography. Sequential left ventricular ejection fraction, normalized left ventricular ejection rate, and regional wall motion. *Circulation* 56:820–829, 1977
15. Dymond DS, Elliott A, Stone D, et al: Factors that affect the reproducibility of measurements of left ventricular function from first-pass radionuclide ventriculograms. *Circulation* 65:311–322, 1982

The Journal of NUCLEAR MEDICINE

High Count Rate First-Pass Radionuclide Angiography Using a Digital Gamma Camera

Rami Gal, Raymond P. Grenier, John Carpenter, Donald H. Schmidt and Steven C. Port

This article and updated information are available at:
http://jnm.snmjournals.org/content/27/2/198

Information about reproducing figures, tables, or other portions of this article can be found online at:
http://jnm.snmjournals.org/site/misc/permission.xhtml

Information about subscriptions to JNM can be found at:
http://jnm.snmjournals.org/site/subscriptions/online.xhtml

SNMMI | SOCIETY OF NUCLEAR MEDICINE AND MOLECULAR IMAGING